Proceedings of 20th International Congress on Acoustics, ICA 2010

23-27 August 2010, Sydney, Australia

Stability Analysis of Broadband Active Noise Equalization Algorithm

Chuansheng Xiao, Fengyan An, Hongling Sun, Jian Xu and Xiaodong Li

Key Laboratory of Noise and Vibration Research, Institute of Acoustics, Chinese Academy of Sciences, 100190 Beijing, China

PACS: 43.50.Ki

ABSTRACT

Broadband active noise equalization algorithm is utilized to shape the noise spectrum in order to match human preference. The stable condition of the algorithm is studied in this paper. Analysis shows that the phase shift of the shaping filter, whose magnitude response defines the desired noise spectrum, has a significant effect on the stability of the system. The stable range of the secondary path modeling phase error is larger than 180° if the phase shift of the shaping filter is between -90° and 90°, and smaller than 180° if it is out of the range. Such result suggests that a shaping filter with a phase response between -90° and 90° can achieve the desired noise spectrum with better stability. Simulations are presented to validate the conclusions.

INTRODUCTION

Active Noise Control (ANC) is a technique that reduces noise by adding noise with opposite phase, which is very effective in attenuating low frequency noise. Different from ANC that aims at minimizing noise, Active Noise Equalization (ANE), or known as Active Sound Quality Control, or Active Sound Profiling, is utilized to change the spectrum of the residual noise to a desired shape. It can be used to retain the wanted sound to a suitable level, or to change the noise spectrum to match human preference.

ANE algorithm is actually derivative of the filtered-X least mean square (FXLMS) algorithm which has been widely used in ANC 0. In ANE, a pseudo-error other than the residual noise picked by the error microphone is minimized. Kuo 错误！未找到引用源。 first proposed the time domain ANE algorithm and later the frequency-domain version 0. Gonzalez 0 and Diego 0 reported the application of the algorithm to reshape multifrequency noise.

The effect of secondary path modelling error on the stability of the algotithm, a practical problem in active control of sound, has been extensively studied in narrowband ANE. It causes the residual noise level deviate from the desired value, known as misequalization 0. It is also a major factor that affects the system convergence and stability 0. The phase scheduled command FXLMS (PSC-FXLMS) algorithm, a new narrowband ANE algorithm proposed by Rees and Elliott 0 , circumvents the misequalization problem and has better stability. Nevertheless, to the best of the authors' knowledge, no research on the stability of broadband ANE has been reported. The shaping filter in the algorithm introduces different gain and phase shift at different frequencies. While in narrowband ANE, no phase shift is introduced. This is the major difference between them.

The paper is organized as follows. In Section 2, the stable condition of the broadband ANE system is derived. Investigation of the condition in Section 3 shows that the phase shift of the shaping filter has a significant impact on the system stability. The stable range of the secondary path modeling phase error is larger than 180° if the phase shift of the shaping filter is between -90° and 90°, and smaller than 180° if it is out of the range. Numerical simulations are presented in Section 4 to demonstrate the results yield from the analysis. Conclusion and further work are stated in Section 5.

STABLE CONDITION OF BROADBAND ANE ALGORITHM

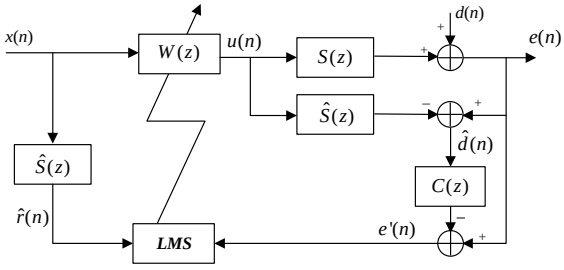

Figure 1. Block diagram broadband ANE algorithm

The block diagram of the broadband ANE algorithm is shown in Figure 1, where $W(z)$ is the adaptive control filter; $S(z)$ and $\hat{S}(z)$ are the secondary path and its model; $C(z)$ is the shaping filter, whose magnitude response defines the desired spectrum of the residual noise. $x(n)$, $u(n)$, $d(n)$ and $e(n)$ are the reference signal, control signal, primary noise and residual noise respectively; $\hat{d}(n)$ is the estimated primary noise, $\hat{r}(n)$ is the filtered reference signal, $e'(n)$ is the pseudo-error signal that need to be minimized by the adaptive control filter. An adaptive control filter with I taps can be updated using FXLMS algorithm:

$$\mathbf{w}(n+1) = \mathbf{w}(n) - \mu e'(n)\hat{\mathbf{r}}(n), \quad (1)$$

where μ is the step size of the adaptation process, $\mathbf{w}(n)=[w_0(n) \quad w_1(n) \quad \cdots \quad w_{I-1}(n)]^T$ is the filter weights, $\hat{\mathbf{r}}(n)=[\hat{r}(n) \quad \hat{r}(n-1) \quad \cdots \quad \hat{r}(n-I+1)]^T$ is the vector of past values of $\hat{r}(n)$, and superscript T denotes transpose of the vector.

The stability of the algorithm is analyzed in the frequency domain. Suppose the complex amplitudes of the reference signal and primary noise at frequency ω are represented as X_ω and D_ω, then the residual noise and pseudo-error signal can be written as

$$E_\omega(n) = D_\omega + S_\omega W_\omega(n) X_\omega, \tag{2}$$

$$E'_\omega(n) = E_\omega(n) - C_\omega[E_\omega(n) - \hat{S}_\omega W_\omega(n) X_\omega], \tag{3}$$

where $W_\omega(n)$, C_ω, S_ω and $\hat{S}_\omega$ are the frequency responses at ω of the respective filters. When $E'_\omega(n)=0$, the control filter and the residual noise converges to

$$W_\omega(\infty) = -\frac{(1-C_\omega)D_\omega}{[S_\omega + (\hat{S}_\omega - S_\omega)C_\omega]X_\omega}, \tag{4}$$

$$E_\omega(\infty) = \frac{\hat{S}_\omega C_\omega D_\omega}{S_\omega + (\hat{S}_\omega - S_\omega)C_\omega}. \tag{5}$$

If there is no modelling error, i. e., $\hat{S}_\omega = S_\omega$, then the spectrum of the residual noise satisfies:

$$|E_\omega(\infty)|^2 = |C_\omega|^2 |D_\omega|^2, \tag{6}$$

and the goal to shape the residual noise is attained. The pseudo-error signal can be represented by the convergent value of the control filter as

$$E'_\omega(n) = [S_\omega + (\hat{S}_\omega - S_\omega)C_\omega][W_\omega(n) - W_\omega(\infty)]X_\omega. \tag{7}$$

The control filter is updated in the frequency domain according to

$$W_\omega(n+1) = W_\omega(n) - \mu E'_\omega(n)\hat{S}^*_\omega X^*_\omega. \tag{8}$$

Substitute Eq. (7) into Eq. (8), and define the difference between the current adaptive filter weight and its convergent value as $\Delta W_\omega(n) = W_\omega(n) - W_\omega(\infty)$, then Eq. (8) is turned into

$$\Delta W_\omega(n+1) = \{1 - \mu|X_\omega|^2 \hat{S}^*_\omega[\hat{S}_\omega + (\hat{S}_\omega - S_\omega)C_\omega]\}\Delta W_\omega(n). \tag{9}$$

Suppose the relationship between the secondary path and its model is represented by

$$\hat{S}_\omega = a_\omega e^{j\theta_\omega} \cdot S_\omega. \tag{10}$$

where a_ω and θ_ω are the magnitude and phase error, then the convergence of $W(z)$ requires that

$$\left|1 - \mu|X_\omega|^2 |S_\omega|^2 a_\omega e^{-j\theta_\omega}[1 + (a_\omega e^{j\theta_\omega} - 1)C_\omega]\right| < 1. \tag{11}$$

Note that μ, a_ω, $|X_\omega|^2$ and $|S_\omega|^2$ are all positive real. If μ is small enough, then the algorithm is stable when the following condition sustains:

$$\mathrm{Re}\{e^{-j\theta_\omega}[1 + (a_\omega e^{j\theta_\omega} - 1)C_\omega]\} > 0. \tag{12}$$

where Re{} denotes the real part of the complex number. Thus a strict stable condition of broadband ANE algorithm is that Eq. (12) is satisfied for all frequencies. In Eq. (12) one can see that different from ANC whose stability depends on the phase error of secondary path model solely, stability of ANE is determined not only by the magnitude and phase error of the model, but also the gain and phase shift introduced by the shaping filter.

DISCUSSION OF THE STABLE CONDITION

Eq. (12) can reveal whether an ANE system is stable under specific modelling error. Now we will investigate the relationship between the shaping filter and the stable modelling error range.

Let $C_\omega = ce^{j\theta_c}$, then Eq. (12) can be transformed into a trigonometry form as

$$(c\cos\theta_c - 1)\cos\theta_\omega + c\sin\theta_c \sin\theta_\omega < a_\omega c\cos\theta_c. \tag{13}$$

Define

$$\phi = \tan^{-1}\frac{c\sin\theta_c}{c\cos\theta_c - 1} + \mathrm{sgn}(c\cos\theta_c - 1)\cdot\pi, \tag{14}$$

where $\mathrm{sgn}(x) = \begin{cases} 0 & x \ge 0 \\ 1 & x < 0 \end{cases}$. Then we can calculate the range of ϕ, which is $\phi \in (-90°, 90°) \cup (90°, 270°)$, and Eq. (13) can be simplified as Eq. (15) according to the property of trigonometry function:

$$\cos(\theta_\omega - \phi) < \frac{a_\omega c\cos\theta_c}{\sqrt{c^2 - 2c\cos\theta_c + 1}}. \tag{15}$$

Eq. (15) implies that the range of θ_ω is significantly varied by θ_c. If $-90° < \theta_c < 90°$, then the right side of Eq. (15) is larger than 0. So the range of $\theta_\omega - \phi$ that satisfies Eq. (15) is larger than $180°$. And since ϕ is a constant determined by the shaping filter, so the range of θ_ω is also larger than $180°$. On the other hand, if $90° < \theta_c < 270°$, then the right side of Eq. (15) is smaller than 0, and the range of θ_ω that satisfies the inequality is smaller than $180°$. When c = 0.5, the relationship between the stable phase error range and a_ω under various phase shift is shown in Figure 2.

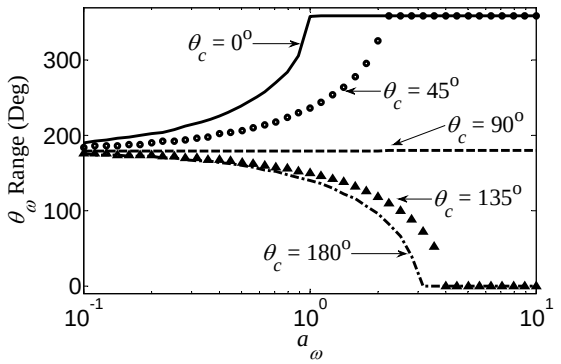

Figure 2. Relation between θ_ω range and a_ω when c = 0.5

One can see that for a given desired gain, a smaller shaping filter phase shift guarantees better stability at the same magnitude error. In the case of $-90° < \theta_c < 90°$, the stable phase error range increases as the magnitude of the model increases. And as it gets large enough, the algorithm can be stable if subjected to any phase error. However, the $90° < \theta_c < 270°$ case goes toward the opposite trend. Large model magnitude will result in a system impossible to be stable. The θ_ω range

is almost the same for both cases when the model magnitude is small, which approaches 180° as a_ω gets smaller.

NUMERICAL SIMULATIONS

In the simulations presented in this section, two shaping filters, $C_{\max}(z)$ and $C_{\min}(z)$, are considered. Their transfer functions are

$$C_{\max}(z) = [0.36 - 1.2\cos(\frac{1}{6}\pi)z^{-1} + z^{-2}]\cdot [0.64 - 1.6\cos(\frac{5}{6}\pi)z^{-1} + z^{-2}], \quad (16)$$

$$C_{\min}(z) = [1 - 1.2\cos(\frac{1}{6}\pi)z^{-1} + 0.36z^{-2}]\cdot [1 - 1.6\cos(\frac{5}{6}\pi)z^{-1} + 0.64z^{-2}], \quad (17)$$

$C_{\max}(z)$ is a maximum phase filter with two pairs of zeros outside the unit circle, and $C_{\min}(z)$ is its minimum phase counterpart. Their magnitude responses are depicted in Figure 3, and phase responses in Figure 4.

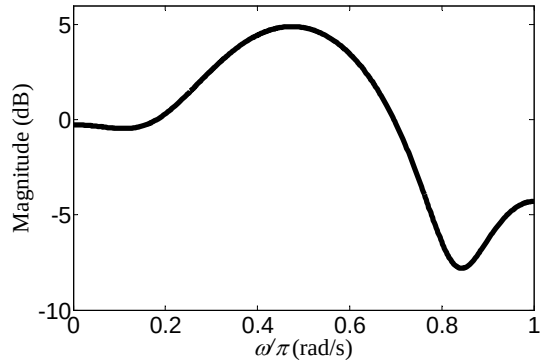

Figure 3. Magnitude response of $C_{\max}(z)$ and $C_{\min}(z)$, which are the same

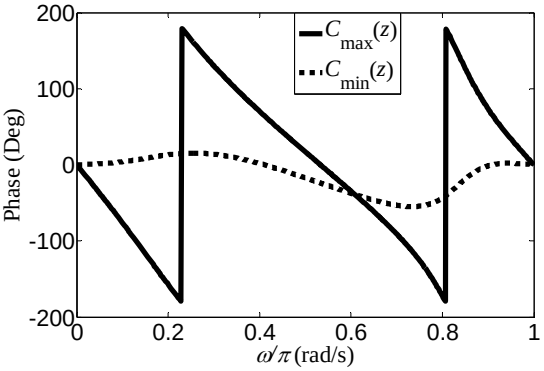

Figure 4. Phase response of $C_{\max}(z)$ and $C_{\min}(z)$

Two simulations are presented here. First, the stable condition of broadband ANE as shown in Eq. (12) is validated. Then according to the discussion of the stable condition, we will compare the stability when $C_{\max}(z)$ and $C_{\min}(z)$ are used as the shaping filter.

Validation of the stable condition

The impulse response of the secondary path used in the simulation is shown as Figure 5. Suppose the magnitude of the secondary path model is 20dB smaller than the actual path and there is no phase error, that is, $a_\omega = 0.01$ and $\theta_\omega = 0°$. $C_{\max}(z)$ is used as the shaping filter in this simulation. In such circumstance, the relationship between the frequency ω and the value of $\mathrm{Re}\{e^{-j\theta_\omega}[1+(a_\omega e^{j\theta_\omega}-1)C_\omega]\}$ is given in Figure 6. Judging by Eq. (12), the algorithm is not stable in the $[0.42\pi \quad 0.62\pi]$rad/s frequency band.

The reference signal is generated by passing the white noise through a fourth order Butterworth bandpass filter whose passband is $[0.42\pi \quad 0.62\pi]$rad/s . After running 1000 simulations, the ensemble average of the pseudo-error signal $e'(n)$ can be calculated, as shown in Figure 7. Convergence is not possible when using a positive step size, but is witnessed if it is a negative one. Since the step size is positive when the model matches the actual path, this result means the algorithm is not stable, which conforms to the prediction by Eq. (12). So, the stable condition in Eq. (12) is capable to judge whether the algorithm is in a stable state.

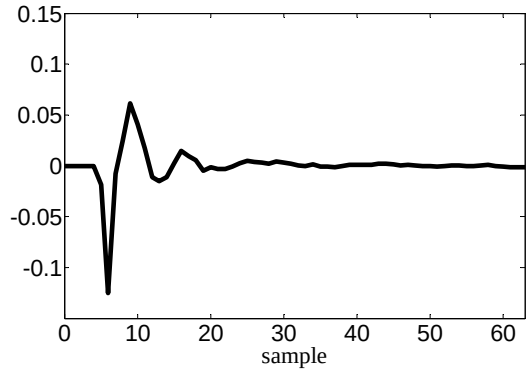

Figure 5. Impulse response of the secondary path

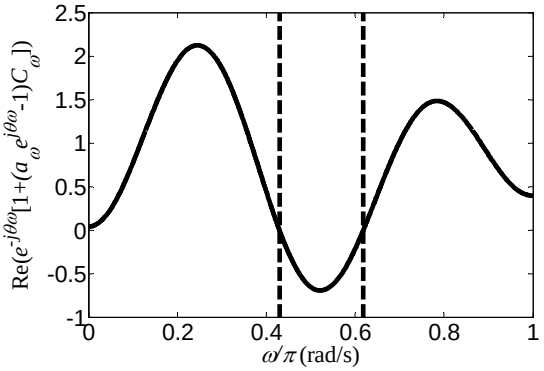

Figure 6. Value of $\mathrm{Re}\{e^{-j\theta_\omega}[1+(a_\omega e^{j\theta_\omega}-1)C_\omega]\}$ for all frequencies when $C_{\max}(z)$ is the shaping filter.

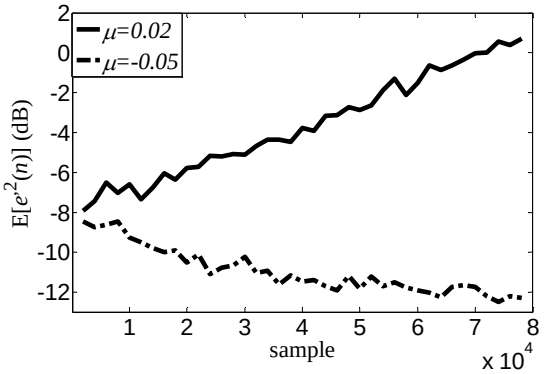

Figure 7. Ensemble average of the pseudo-error $e'(n)$

Stability comparision when using $C_{\max}(z)$ and $C_{\min}(z)$ as the shaping filter

The stability of using $C_{\max}(z)$ and $C_{\min}(z)$ as the shaping filters is compared here. These two filters have the same magni-

tude response, so if there is no modelling error, both of them will result in the same desired residual noise spectrum. However, they differ drastically in phase response. The phase shift of $C_{max}(z)$ exceeds the $(-90°, 90°)$ bound around 0.2π rad/s and 0.8π rad/s, while $C_{min}(z)$ stays in the bound for all frequencies. According to the analysis of the stable condition, $C_{min}(z)$ can tolerate larger modelling error and is more stable than $C_{max}(z)$.

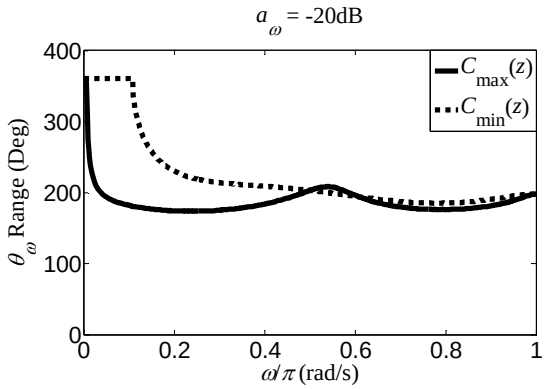

Figure 8. Range of stable modelling phase error θ_ω when magnitude error a_ω is -20dB

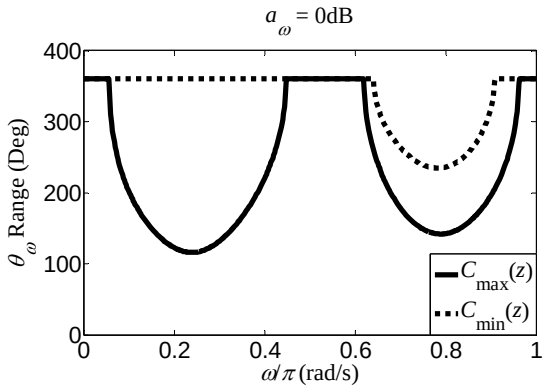

Figure 9. Range of stable modelling phase error θ_ω when magnitude error a_ω is 0dB

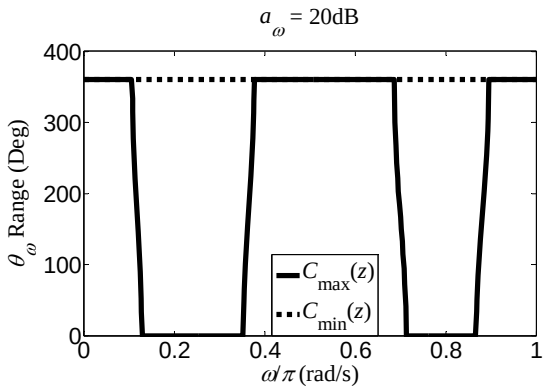

Figure 10. Range of stable modelling phase error θ_ω when magnitude error a_ω is 20dB

Figure 8 to Figure 10 compares the range of the stable modelling phase error θ_ω when different shaping filter is used. When the magnitude of the model is 20dB smaller than the actual path, the range of θ_ω is larger when $C_{min}(z)$ is used as the shaping filter at low frequency. When the magnitude of the model is the same with the path, at the frequency between $[0 \quad 0.6\pi]$ rad/s, the algorithm can tolerate any phase error when $C_{min}(z)$ is used. While the range of θ_ω shrinks drastically between the $[0.05\pi \quad 0.45\pi]$ rad/s frequency range if $C_{max}(z)$ is the shaping filter. The difference is even more evident when the magnitude of the model is 20dB larger than the path. In this case, $C_{min}(z)$ can guarantee absolute stability. While there is no way to stablize the algorithm at the frequency range of $[0.15\pi \quad 0.35\pi]$ rad/s and $[0.7\pi \quad 0.9\pi]$ rad/s when $C_{max}(z)$ is used.

Figure 11 depicts the distribution of stable modelling phase error θ_ω when the magnitude of the model is 20dB smaller than the actual path and $C_{max}(z)$ is the shaping filter, while Figure 12 shows the $C_{min}(z)$ case. Non-stable phase error is shown in black and stable phase error is shown in white. Comparing these two figures, one can see that the two shaping filters have similar distribution, except in the low frequency range.

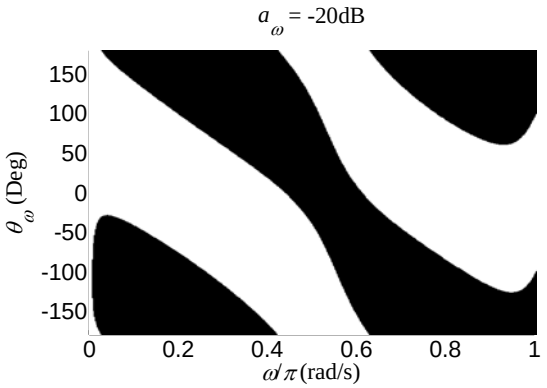

Figure 11. Distribution of stable modelling phase error θ_ω when magnitude error a_ω is -20dB and $C_{max}(z)$ is the shaping filter.

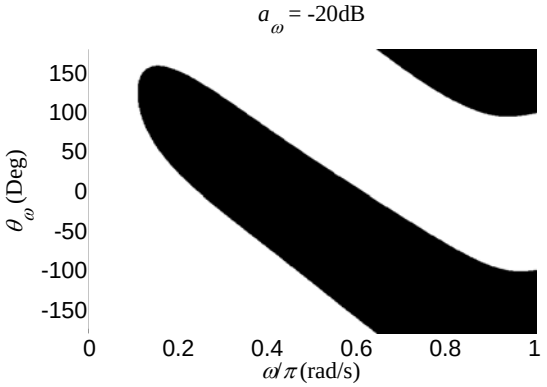

Figure 12. Distribution of stable modelling phase error θ_ω when magnitude error a_ω is -20dB and $C_{min}(z)$ is the shaping filter.

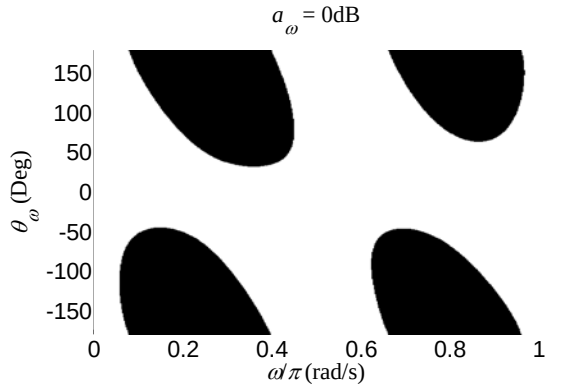

Figure 13. Distribution of stable modelling phase error θ_ω when magnitude error a_ω is 0dB and $C_{\max}(z)$ is the shaping filter.

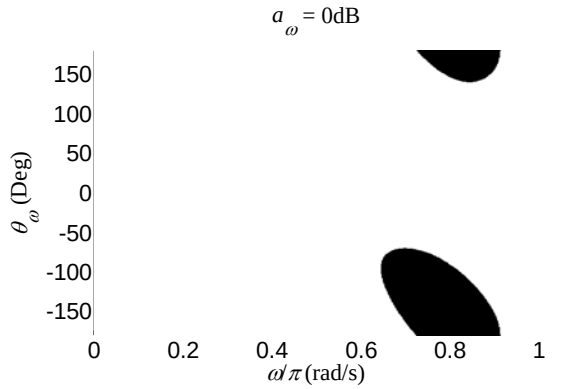

Figure 14. Distribution of stable modelling phase error θ_ω when magnitude error a_ω is 0dB and $C_{\min}(z)$ is the shaping filter.

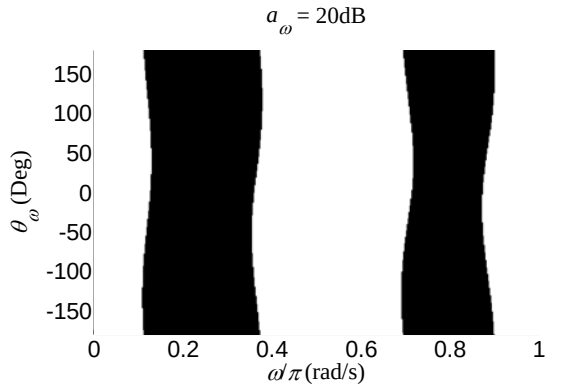

Figure 15. Distribution of stable modelling phase error θ_ω when magnitude error a_ω is 20dB and $C_{\max}(z)$ is the shaping filter.

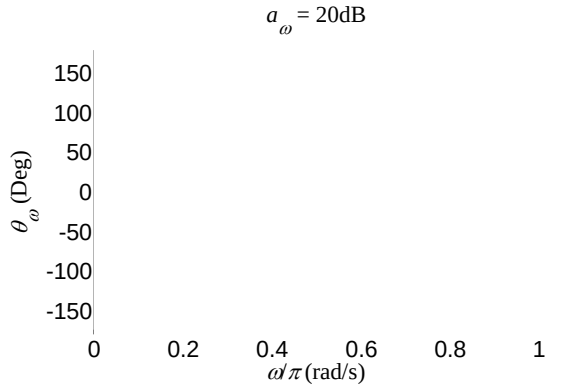

Figure 16. Distribution of stable modelling phase error θ_ω when magnitude error a_ω is 20dB and $C_{\min}(z)$ is the shaping filter.

Figure 13 and Figure 14 depict the distribution of stable modelling phase error θ_ω when the magnitude of the model is the same with the actual path, where $C_{\max}(z)$ and $C_{\min}(z)$ are used as the shaping filter respectively. Figure 15 and Figure 16 shows the cases when the magnitude of the model is 20dB larger than the actual path. These figures confirm that a shaping filter whose phase shift is within the $(-90°, 90°)$ bound can guarantee better stability to the ANE algorithm.

CONCLUSIONS

The stable condition of broadband ANE algorithm is derived and analyzed in this paper. Such condition is strict enough to assure correct judgment of whether the algorithm is stable when secondary path modelling error occurs. Analysis of the condition shows that the stable modelling error range is larger for a shaping filter whose phase shift lies within the $(-90°, 90°)$ bound. That means a shaping filter with the desired magnitude response and a phase response between $(-90°, 90°)$ can achieve the control objective with better stability. Further work will focus on designing such shaping filter with specified magnitude response.

REFERENCES

1 S. J. Elliott, *Signal Processing for Active Control*. (Academic Press, London, 2001) pp. 132-149.

2 S. M. Kuo and Y. Yang, "Broadband adaptive noise equalizer", *IEEE Signal Processing Letters*, **3**(8), 234-235 (1996).

3 S. M. Kuo, R. K. Yenduri and A. Gupta, "Frequency-domain delayless active sound quality control algorithms", *Journal of Sound and Vibration*, **318**(4-5), 715-724 (2008).

4 A. Gonzalez, M. de Diego, M. Ferrer and G. Piñero, "Multichannel active noise equalization of interior noise", *IEEE Transaction on Audio, Speech and Language Processing*, **14**(1), 110-122 (2006).

5 M. Diego, A. Gonzalez, M. Ferrer and G. Piñero, "Multichannel active noise control system for local spectral reshaping of multifrequency noise", *Journal of Sound and Vibration*, **274**(1-2), 249-271 (2004).

6 L. Wang and W. S. Gan, "Analysis of misequalization in a narrowband active noise equalizer system", *Journal of Sound and Vibration*, **311**(3-5), 1438-1446 (2008).

7 L. Wang and W. S. Gan, "Convergence analysis of narrowband active noise equalizer system under imperfect secondary path estimation", *IEEE Transaction on Audio, Speech and Language Processing*, **17**(4), 565-571 (2009).

8 L. E. Rees and S. J. Elliott, "Adaptive algorithms for active sound-profiling", *IEEE Transaction on Audio, Speech and Language Processing*, **14**(2), 711-719 (2006).